Journal of
Membrane Science & Technology

Visa and Popa, J Membra Sci Technol 2015, 5:1
DOI: 10.4172/2155-9589.1000133

Research Article Open Access

Adsorption of Heavy Metals Cations onto Zeolite Material from Aqueous Solution

Maria Visa[1]* **and Nicoleta Popa**[2]

[1]*Department of Renewable Energy Systems and Recycling, Transilvania University of Brasov, Romania*
[2]*Department of Forest District Teliu, National Administration of State Forests Romsilva, Romania*

Abstract

Increased urbanization and industrialization led to excessive release of wastes into the environment; one of them, causing many problems not only to the environment but also to human health, is fly ash resulted from coal combustion. One of the solutions for solving these problems would be fly ash reutilization as an adsorbent for wastewater treatment and for obtaining new and efficient materials such as zeolites. Class "F" fly ash collected from C.H.P. Craiova from Romania was used for obtaining new zeolite materials for advanced wastewater treatment. This material was characterized by AFM, XRD, FTIR, SEM to outline the crystalline and morphology modifications. Hydrothermal modified fly ash using NaOH was used for heavy metals removal (Cd^{2+}, Cu^{2+} and Ni^{2+}) from synthetic wastewaters containing one, two and three pollutants. For obtaining a maximum efficiency during the adsorption process the adsorption conditions (contact time, optimum amount of substrate) were optimized. These parameters were further used in thermodynamic and kinetic modeling of the adsorption processes. The uptake of Cd^{2+}, Cu^{2+} and Ni^{2+} was followed by a Langmuir adsorption isotherm and the maximum uptake capacity was estimated to be 95.24 mg/g Cd^{2+}, 107.52 mg/g Cu^{2+} from aqueous solution with two cations. Correlated with the surface structure, composition and morphology the adsorption kinetic mechanisms and the substrate capacities are further discussed.

Keywords: Heavy metals; Adsorption; Filtration; Zeolite; Wastewater treatment

Introduction

The pollution of water is one big problem in each country. More hundred pollutants are released every day into the environment from numerous branches of industries. The main industries responsible for large amount of wastewater with complex pollutant load are: the mining and extractive industry, electroplating and metal surface treatment processes, metallurgy, metal coating and plastics. Water interaction with chemical substances resulting wastewaters with a large quantities of heavy metals, different organic or inorganic pollutants and the last target are ecosystem and the health of humans.

Many compounds of heavy metals are easy soluble in water and can be adsorbed by living organisms part of the food chain. Some heavy metals (copper, cobalt, iron, manganese, vanadium, strontium and zinc) are accepted in small concentration for living organisms but excessive levels of essential metals can be detrimental to the organisms. Non–essential heavy metals (including cadmium, lead and zinc) are dangerous for living organisms [1,2].

Heavy metals are persistent pollutants, non-biodegradable and can be accumulated easily in organisms even at low concentrations, causing serious illness; common effects on humans are described as: increased salivation, severe stomach irritations leading to vomiting and diarrhea, abdominal pain, choking, high blood pressure, iron-poor blood, liver disease, pancreas and nerve or brain damage, poisoning by ingestion include vomiting, vomiting of blood, hypotension, coma, jaundice, and gastrointestinal pain [3,4]. For avoiding flora, fauna and health problems, the discharge limits are strict and require advanced wastewater treatment processes [5,6].

On the other hand the heavy metals can deactivate the active sludge (poisoning the bacteria) from the secondary treatment plants; therefore the chemical treatment must remove heavy metals before the biological step.

The conventional techniques used for heavy metal removal are expensive and with average efficiency. The most common and widely used methods for advanced heavy metal removal are: chemical precipitation, flotation, flocculation, sedimentation, solvent extraction, oxidation/reduction and dialysis/electro-dialysis, reverse osmosis, ultra filtration, electrochemical deposition, ion exchange and adsorption e.g.

Choosing one or more complex solutions is subject of efficiency and cost analysis reported at large quantity of wastewater. Among these, adsorption technologies have several advantages: easy operation and well known technology, inexpensive equipment, less sludge, adsorbents' reuse after desorption. In water the heavy metals cations are hydrated with different bipolar water molecules.

Heavy metals (cadmium, copper, zinc, nickel) removal by adsorption was reported on, sugar beet pulp [7], bituminous coal, peat [8], clay and diatomite [9] natural zeolite [10] or on zeolite obtained by conversion of fly ash [11].

This paper presents the synthesis, characterization and results of adsorption of zeolite ZCR40 obtained from fly ash by hydrothermal method, which were used as adsorbents in removal of Cd^{2+}, Cu^{2+} and Ni^{2+} from mono-, di-, and three-component systems.

Materials and Methods

Raw Fly Ash was collected from the electrostatic filters in the

---

***Corresponding author:** Maria Visa, Department of Renewable Energy Systems and Recycling, Transilvania University of Brasov, Eroilor 29, 500036 Brasov, Romania, Tel: 0040-729109355; Fax: 0040-268-410525; E-mail: maria.visa@unitbv.ro

Received May 04, 2015; **Accepted** July 13, 2015; **Published** July 16, 2015

Citation: Visa M, Popa N (2015) Adsorption of Heavy Metals Cations onto Zeolite Material from Aqueous Solution. J Membra Sci Technol 5: 133. doi:10.4172/2155-9589.1000133

combined heat and power plant S.E. Craiova II, Romania. The content of the main constituents are presented in Table 1.

The total percentage of SiO_2, Al_2O_3 and Fe_2O_3 is 78.37% (above 70%),thus, according the ASTM C618 classification, the fly ash –S.E.Craiova II., is of class F [12].

Fly ash was washed in ultra-pure water by stirring up (100 rpm), at room temperature, for 48h, to remove the soluble compounds, until constant pH was reached, at the value of 11.5. The water resulted after washing FA had an ionic conductivity of K=630 [µS/cm] and a TDS value of 640 mg/L, as result of the soluble compounds dissolution: CaO, MgO, Na_2O, K_2O. The dry fly ash was subject sieving to determine the size distribution Table 2.

The zeolite materials were obtained from washed fly ash (FACRw) with 40 µm granulometry by mixed with NaOH solution 3N in autoclave for 5h at 150°C. The fractions >40 µm can be used for obtaining geo-polimers, for cement, bricks, stone blocks. After running time the material was washed with ultra-pure water till constant pH, filtrated, dried at 105-120°C overnight and was analyzed. This new material denoted (ZCR40) was used in adsorption experiments.

The crystalline structures of the FAw and ZCR40 were evaluated by XRD (Bruker D8 Discover Diffractometer). The AFM images (Ntegra Spectra, MT-NDTmodel BL222RNTE) were used for surface morphology studies. The AFM was used to characterize the uniformity, grain size and pores size distribution of the zeolite material. Image analysis was carried out by means of WSxM software, to evaluate the pore size distribution [13]. By using scanning electron microscopy (SEM, S-3400N– Hitachi) further surface investigations were done at an accelerating voltage of 20 kV. Surface compositions of zeolite ZCR40 was measured before and after adsorption using energy dispersive X-ray spectroscopy (EDS Thermo Scientific Ultra Dry). By using porosity analysis and BET surface (Autosorb-IQ-MP, Quantachrome Instruments) characterization of the surface was completed.

The new substrates (ZCR40) were used in adsorption experiments for removing heavy metals from synthetic wastewater loaded with Cd^{2+}, Cu^{2+} and Ni^{2+} cations.

Adsorption experiments

Batch adsorption experiments were carried out under mechanical stirring, at room temperature 20-22°C considering that the vapors pressure of water at this temperature is low (0.023-0.024 bar), thermosetting was not necessary.

Three series of experimental test of adsorption were done:

Adsorption on ZCR40 substrate in solution containing one, two and three pollutants:

Compound	% in FA	Compound	% in FA	Compound	% in FA
SiO_2	46.13	MgO	5.24	MnO	-
Al_2O_3	21.39	K_2O	0.5-2	P_2O_5	-
Fe_2O_3	10.85	Na_2O	0.2-0.6	LOI*	-
CaO	10.65	TiO_2	<1%	SiAlFe**	78.37

Table 1: The composition of fly ash (FA) - C.H.P. Craiova [%].

Raw FA S.E. Craiova II	Particle size distribution [%]			
	20 µm	40 µm	100 µm	<100 µm
	5.2	53.5	31.8	9.5

Table 2: Particle size distribution [%].

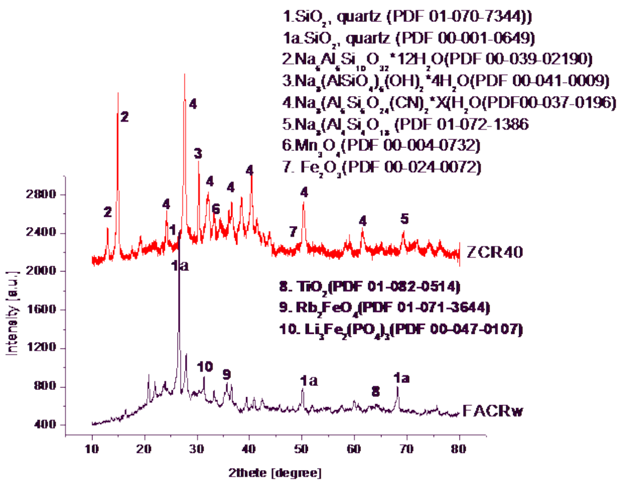

Figure 1a: XRD data.

- Cd^{2+}/Cu^{2+} from mono-cationic system, under mechanical stirring;
- Cd^{2+} + Cu^{2+} from di-cationic system, under mechanical stirring;
- Cd^{2+}, Cu^{2+} and Ni^{2+} from three-cationic system, under mechanical stirring.

In all experiments, the pollutant systems were synthetically prepared using bidistilled water and $CdCl_2$*2.5 H_2O (Scharlau Chemie S.A., c<98%), $CuCl_2$*2H_2O (Scharlau Chemie S.A., c<98%) and $NiCl_2$*6H_2O (Scharlau Chemie S.A., c<98%). The experiments were done using heavy metals solutions in concentration of range of C_{Cd2+}= 0.560 mg/L, C_{Cu2+}=0.330 mg/L and C_{Ni2+}=0.300 mg/L.

The optimal contact time was evaluated in suspension, 0.1 g ZCR40 in 50 mL of equimolar multi-cation solutions of cadmium, copper and nickel; aliquots were taken at certain moments (10, 15, 30, 45, 60, 90, 120, 150 and 180 min), when stirring was briefly interrupted and after filtration the volumes of supernatant were analyzed. The residual metal concentration in the aqueous solution was analyzed by AAS (Analytic Jena, ZEEnit 700), at λ_{Cd}=228.8 nm, λ_{Cu}=324.75 nm and λ_{Ni}=232.00 nm. The working pH was in the range of 5.4-6.3. Preliminary experiments proved that heavy metal losses due to the adsorption to the container walls and to the filter unit 0.22 µm were negligible.

Results and Discussion

Characterization of the substrates

The composition of silicon-aluminous of the fly ash is confirmed by XRD spectra, Figure 1. The major crystalline components of raw fly ash are: αSiO_2 (quartz) identified by the sharp peaks in the range of $2\theta = 26^o$ and hematite (Fe_2O_3).

The diffractogram (Figure 1) data show that some compounds: SiO_2 (quartz), $Li_3Fe_2(PO_4)_3$ (lithium iron phosphate), $Rb_2(FeO_4)$ (rubidium iron oxide) from FACRw are or not presented in low percentage, while the percent of sodium aluminum hydrate ($Na_6Al_6Si_{10}O_{32}$*12H_2O), sodium aluminum hydroxide hydrate ($Na_8(AlSiO_4)_6$*$(OH)_2$*4H_2O) sodium aluminum cyamide hydrare (($Na_8Al_6Si_{10}O_{24}$ $(CN)_2$*xH_2O),) sodium aluminum silicate hydrate $Na_8(AlSiO_4)_6$*4H_2O and other phases of the aluminosilicates typical the zeolites is increased in the zeolite material (ZCR40). The quartz syn, hematite and manganese oxide are in small proportion. The area picks of new alumino-silicates phases are higher. The hydrothermal process of FACRw further promotes the surface interactions, including dissolution, re-crystallization processes that confirm chemical restructuring. The crystalline phases increased from 38.5% at 51.1% for ZCR40.

An evaluation criterion of raw fly ash into zeolites can be the proportion of quartz from raw fly ash converted to aluminosilicates using equation (1).

$$R = \frac{\%\ \text{quartz in ZCR40}}{\%\ \text{quartz in rawFA}} \qquad (1)$$

R value is low for ZCR40 materials showing high conversion of SiO_2 from FACRw to crystalline zeolite (NaP1) by hydrothermal treatment.

The content of quartz and of mullite was found to be mainly responsible which hinder formation of zeolite and their activity [14-20].

The composition of crystalline phases, crystalline degree, and morphological changes are presented in Table 3.

Other information related to the morphology and characteristics of the surface were obtained from the AFM and SEM micrographs (Figures 2 and 3).

These AFM images were used to characterize the surface morphology: the uniformity, grain size and pore size distribution [19] of the samples Figure 2. The FACRw and ZCR40 have a rough surface

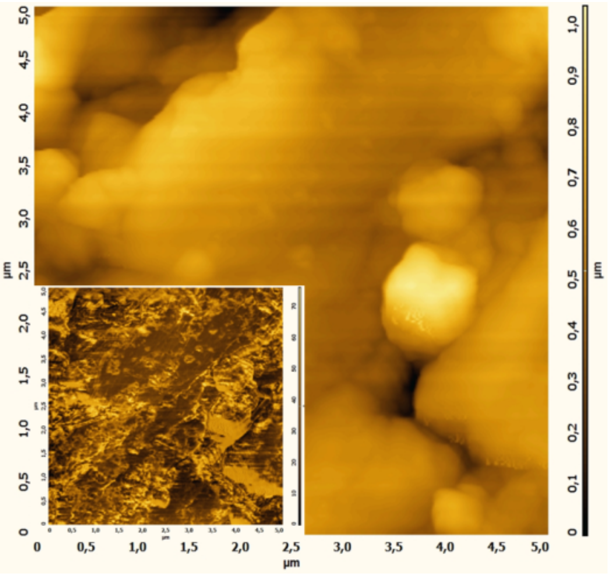

Maximum amplitude = 54.3 nm

Averageroughness = 74.1 nm

Mezo-pori = 265 nm

[Si/Al] = 2.49

Figure 1b: XRD data of FACRw.

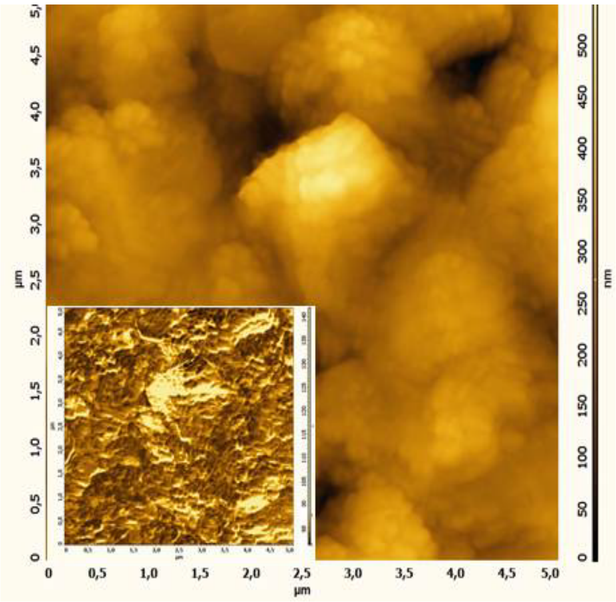

Maximum amplitude = 45.5 nm

Avreageroughnes = 69.4 nm

Mezo-pori = 150 nm

[Si/Al] = 1.37

Figure 1c: XRD data of ZCRs.

Crystalline degree			**Morphology modifications**			
Sample	Composition of crystalline phases	Crystalline degree [%]	R	Specific surface area (BET) [m^2/g]	Micropores volume (t-plot) [cm^3/g]	Average pores diameter [nm]
FACRw	*Quartz, SiO_2, hexagonal (31.6%)* Graphite, hexagonal (4.83%) *Na/K Aluminosilicates /hydrate (57.45%)* Hematite, Fe_2O_3, romboedric (5.65%), Mn_3O_4, tetragonal (0.46%)	38.5	-	4.09	0.004	27.2
ZCR40	Quartz, SiO_2, hexagonal (6,96%); Hematite, Fe_2O_3, romboedhric (2,41%) TiO_2, monoclinic (1.27%) Mn_3O_4, tetragonal (1.56%) Aluminosilicates simple/hydratated de Na/K (87.8%)	58.50.1	0.07	54.09	0,003	17.98

Table 3: The characteristics of the raw fly ashes and of the zeolite material.

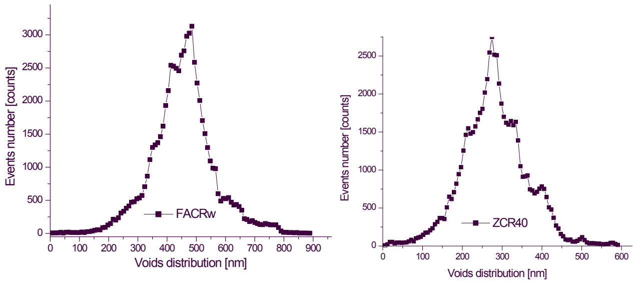

Pore histogram for FACRwPore histogram for ZCR40

RMS roughness =104.52 nm	RMS roughness =80.39 nm
Average roughness = 77.73 nm	Average roughness = 61.47 nm
Average height =459.01 nm	Average height =284.34 nm

Figure 2: AFM topography, average roughness, phase's distribution and pore distribution.

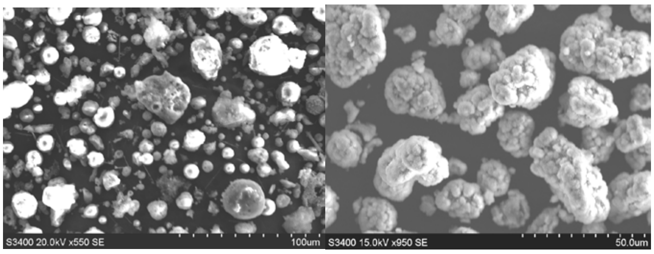

(a) (b)

Figure 3: Scanning Electron Microscopic images (a) FACRw; (b) ZCR40.

Substrate	Surface Energy [mN/m]	Disperse contribution [mN/m]	Polar contribution [mN/m]
ZCR40	22.44	4.17	18.31

Table 4: Surface energy data for the substrates.

with larger pores/voids heterogeneously distributed, confirmed by the pores/voids distribution curves with two or three maxima.

Optimizing fly ash substrate by washing and hydrothermal treating the roughness, RMS roughness show a decrease from 74.1 nm to 45.5 nm, from 284.34 nm to 104.52 nm respectively. The roughness can give information knowing the level of investigation (the millimetric scale usually permits one to distinguish the main surface treatments) [15]. These chemical report (Si/Al) and structural changes are mirrored in morphology modifications, Figures 2a and 2b resulting large differences in the substrates' affinity for heavy metals. On phase's distributions images, it can be seen more agglomerates in the new material adsorbent so more macro-pores and meso-pores are ready to lodge the cations of heavy metals.

The SEM images Figure 3 show significant modifications during the fly ashes processing. Most FACRw particles are spherical and in zeolite materials large agglomerates are formed (Figure 3).

The polar and disperse contributions to the surface energy of ZCR40 was calculated according to the model developed by Owens, Wendt, Robel and Kaelble and are presented in Table 4.

The data show a large polar component, recommending the zeolite ZCR40 as a good adsorption substrate for heavy metals cations.

The zeolite material ZCR40 has composition to zeolites leading to similar types of vibrations. The asymmetric stretch of the Si-O-Si or Si-O-Al bonds corresponds to the peak positioned around 1000 cm^{-1}. Moreover, the water molecules associated with the cations and hydrogen bonded to the oxygen ions of the framework; explain the peak recorded at 1640.38 cm^{-1}, characteristic to the bended mode in the water molecules [16,17]. The characteristic peaks for zeolite are known from the literature [18,19] as being positioned at 421.89 cm^{-1}; 666.03 cm^{-1} and 956.02 cm^{-1}, (Figure 4 and Table 5).

Adsorption of heavy metals on ZCR40 substrate

The adsorption experiments of Cd^{2+}, Cu^{2+} and Ni^{2+} on the zeolite substrate ZCR40 were carried out as a function of contact time, adsorbent dose and heavy metals concentration at optimum contact time. Maximum removal efficiency (η) of Cd^{2+}, Cu^{2+} respectively Ni^{2+} cations was evaluated using the following eqn (2).

$$\eta = \frac{(c^{i}_{HM} - c^{e}_{HM}) \times 100}{c^{i}_{HM}} \qquad (2)$$

where: c^{i}_{HM} - the initial concentration and c^{e}_{HM} - equilibrium momentary concentration of the heavy metals (HM).

Adsorption equilibrium is reached in most cases after 60 min with stabilization at 90 min (Figures 5a, 5b and 5c). These values are acceptable for technology process so each of these materials can be further used for technology transfer.

An important parameter governing the efficiency of the adsorption of heavy metals is the volume of the cation, copper cation (hydrated

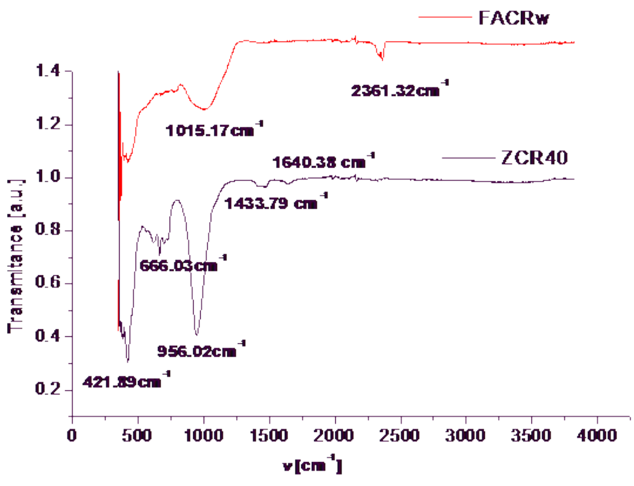

Figure 4: FT-IR spectra of the FACRw and ZCR40.

Compounds	Wavenumber	Allocation
Water	1630…1640	Vibration H - O or H - OH from reaction products hydroalumino-silicate
Kaolin/zeolites	1028…1032	Asymmetric stretching vibration of Si-O-Si bonds
Silicates of Ti/ zeolites	950…961	Asymmetrical stretching vibration of Si-O-Ti /asymmetrical stretching
Feldspars/zeolite	660…670	Symmetric stretching vibration ties Al-O and Si-O
Hematite/zeolite	570…590	Bending Vibration of the links Al-O, Si-O, Al-O-Si and Fe-O
Kaolin/zeolites	400…420	Vibration of the open pores, band O-Si-O

Table 5: IR bands characteristic of the zeolites material.

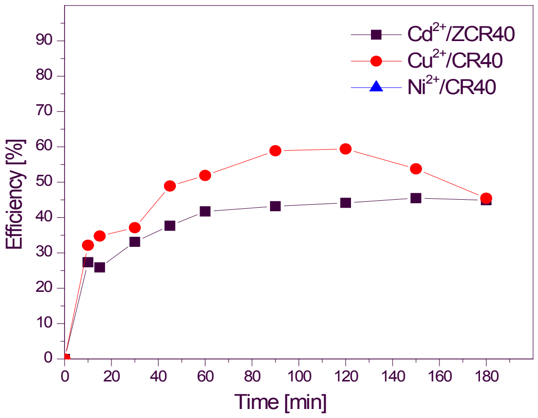

Figure 5a: Efficiency of heavy metals (Cd^{2+}, Cu^{2+}, Ni^{2+}) removal from mono-cationic system on ZCR40.

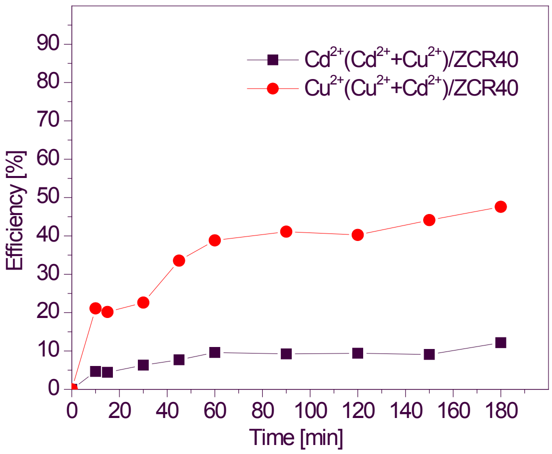

Figure 5b: Efficiency of heavy metals (Cd^{2+}, Cu^{2+}) removal from bi-cationic system on ZCR40.

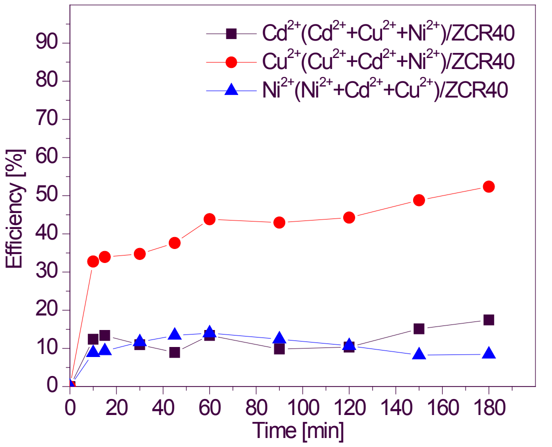

Figure 5c: Efficiency of heavy metals (Cd^{2+}, Cu^{2+}, Ni^{2+}) removal from three-cationic system on ZCR40.

with water molecules 4 .. 6) having the smallest volume. The significant difference observed between single and binary metal adsorption is in the initial metal removal rate. Slightly lower initial metal removal rate observed in the case of binary adsorption is probably due to of competing hydrated metal ions present in solution. The effect amount of ZCR40 vas analyzed and presented in Figure 6.

The maximum of efficiency is obtained after 90 min. in all cases of adsorption and was further used in next experiments. Increasing the amount of ZCR40 substrate will be an increase of amount of active site.

Heavy metals cations can establish bonds with active sites (≡ SiO^-) and (≡ AlO^-) forming complex structure accordind to reaction (3, 4):

$$2\ (\equiv SiO\text{-}) + M^{2+} \rightarrow (\equiv Si\text{-}O)_2\ M \qquad (3)$$

$$2\ (\equiv AlO\text{-}) + M^{2+} \rightarrow (\equiv Al\text{-}O)_2\ M \qquad (4)$$

The effect of concentration of Cd^{2+}, Cu^{2+}, Ni^{2+} solutions on the adsorption was studies at optimal time (90 min.) and optimal mass (0.35 g ZCR40) Figure 7.

High adsorption efficiency for (Cd^{2+}, Cu^{2+}, Ni^{2+}) cations are registration at the concentration up to 0.0003125 val/L.

The adsorption capacity Z (Figure 8) is a function of the initial cation

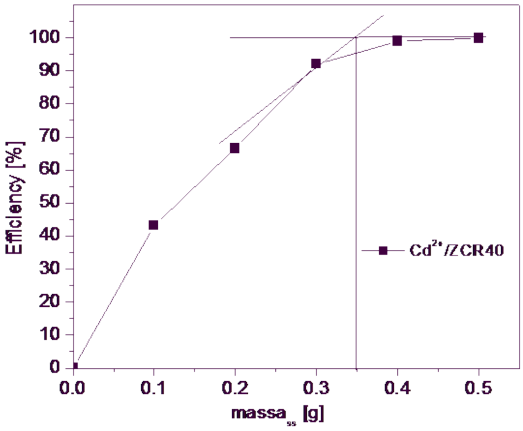

Figure 6: Influence of the amount of CRZ40 adsorbent on the removal efficiency.

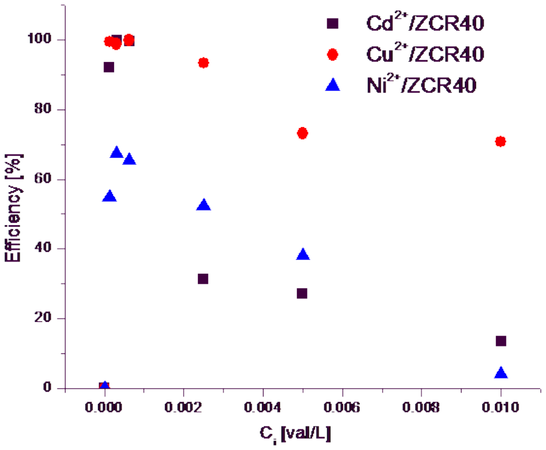

Figure 7: Effect of initial concentration on ZCR40 substrate.

Substrate	**Pseudo- first order kinettics**		**Pseudo-second order kinetics**			**Interparticle diffusion**		
	K_L [min^{-1}]	**R^2**	**k_2 [g/mg·min]**	**q_e [mg/g]**	**R^2**	**K_{id} (mg/gmin$^{1/2}$)**	**C**	**R^2**
Cd^{2+}								
ZCRs 40	0.030	0.964	0.081	129.87	0.996	5.069	63.414	0.844
Cu^{2+}								
ZCR40	0.028	0.904	0.203	86.207	0.928	5.964	22.128	0.928
$Cd^{2+}(Cd^{2+}+Cu^{2})$								
ZCR40	0.021	0.946	0.5156	27.701	0.988	1.717	7.702	0.848
$Cu^{2+}(Cd^{2+}+Cu^{2})$								
ZCR40	0.015	0.907	0.309	81.967	0.983	2.155	9.502	0.906
$Cd^{2+}(Cd^{2+}+Cu^{2+}+Ni^{2+})$								
ZCR40	-	0.229	0.214	36.364	0.892	-	-	0.225
$Cu^{2+}(Cd^{2+}+Cu^{2+}+Ni^{2+})$								
ZCR40	0.012	0.853	0.194	86.957	0.981	3.232	38.904	0.829
$Ni^{2+}(Cd^{2+}+Cu^{2+}+Ni^{2+})$								
ZCR40	-	0.525	0.019	13.316	0.862	-	-	0.192

Table 6: Kinetic parameters of heavy metals adsorption.

concentration, the adsorbent dose, the energy surface of adsorbent (polar contribution) and the nature solute – sorbent interaction.

The adsorption kinetic

The metal uptake q_e (mg/g) was evaluated for the kinetic studies by using the initial and current, t, heavy metal concentrations (c^i_{cation} and c^t_{cation}) in a given solution volume (V=50 mL) for a given amount of ZCR40 (m_s = 0.1 g) as given in eq. (5):

$$q_e = \frac{(c^i_{cation} - c^t_{cation}) \cdot V}{m_s} \tag{5}$$

By using the following equations (6) and (7) the kinetics of the heavy metals adsorption were modeled:

- The pseudo first-order eq. (6) [20]:

$$\log(q_e - q_t) = \log q_e - \frac{K_L}{2.303} t \tag{6}$$

where K_L is the Lagergreen constant, q_e is the equilibrium uptake value and q_t the current metal uptake.

- The pseudo-second order kinetic eq. (7) [21,22]:

$$\frac{t}{q_t} = \frac{1}{k_2 q_e^2} + \frac{t}{q_e} \tag{7}$$

where k_2 is rate constant.

The inter particle diffusion is another possible kinetic model that can be applied in adsorption processes eq. (8), [23].

$$q = k_{id} t^{1/2} + C \tag{8}$$

where k_{id} is rate constant and C is the intercept at the ordinate. If the plot of qt vs. t1/2, according to eq.(8), gives a straight line, then intra particle diffusion was involved in the adsorption process; in addition, if the straight line passes through the origin, then the intra-particle diffusion was the rate-limiting step [24]. Generally, the intercept, C, gives an idea about boundary layer thickness: the larger value of intercept, the greater the boundary layer diffusion effect is shown in Table 6 [25].

The adsorption of Cu^{2+} cation on porous materials from mono-, di- and three-components system can by modeled with all kinetic model presented above, Table 6. These models is based on the assumption that the rate limiting step may be a chemical adsorption involving between the adsorbent (ZCR40) and the adsorbate [12,19].

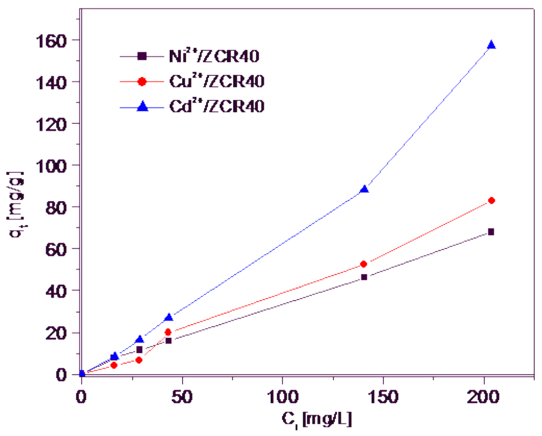

Figure 8: Adsorption capacity versus concentration of the heavy metals.

Adsorption isotherm

The adsorption isotherm data were experimentally obtained based on: the optimized contact time (90 min), the substrate amount (0.35 g ZCR40 in 50 mL suspention). The adsorption parameters were calculated considering the Langmuir and Freundlich equations (9) and (10) [26].

the Langmuir isotherm – linearization:

$$\frac{C_{eq}}{q_{eq}} = \frac{1}{q_{\max} \cdot a} + \frac{C_{eq}}{q_{\max}} \tag{9}$$

- where q_{max} (mg/g) represents the maximum monolayer adsorption capacity, a is a constant related to the adsorption free energy, q_{eq} is the amount of metal ions adsorbed from the solution with the equilibrium concentration, C_{eq}.

the Freundlich isotherm – linearization:

Substrate	**Langmuir Parameters**			**Freundlich Parameters**		
	q_{max} [mg/g]	**a**	**R^2**	**n**	**K_F**	**R^2**
Cd^{2+}						
ZCR40	95.238	0.0004	0.997	-	-	0.285
			Cu^{2+}			
ZCR40	107.527	0.0003	0.917	-	-	0.801
$Cd^{2+}(Cd^{2+}+Cu^{2+})$						
ZCR40	36.764	0.016	0.920	-	-	0.657
$Cu^{2+}(Cd^{2+}+Cu^{2+})$						
ZCR40	53.763	0.001	0.993	-	-	0.660
$Cd^{2+}(Cd^{2+}+Cu^{2+}+Ni^{2+})$						
ZCR40	18.657	0.04	0.978	-	-	0.652
$Cu^{2+}(Cd^{2+}+Cu^{2+}+Ni^{2+})$						
ZCR40	13.774	0.001	0.970	-	-	0.896
$Ni^{2+}(Cd^{2+}+Cu^{2+}+Ni^{2+})$						
ZCR40	26.525	0.066	0.999	-	-	0.665

Table 7: Adsorption isotherm parameters.

$$\ln q_{eq} = \ln k_f + \frac{1}{n}\ln C_{eq} \qquad (10)$$

- where k_f is Freundlich constant, an indicator of the adsorption capacity, and the 1/n dimensionless parameter is a measure of the adsorption density. The adsorption parameters are presented in Table 7.

The Langmuir model fits the equilibrium data much better than the Freundlich model for this adsorbent Table 4. Accordingly with table data the adsorption was rather homogeneous than heterogeneous and rather monolayer than multilayer for all cations studied.

Conclusions

Adsorption efficiency of cadmium, cooper and nickel cations is reduced compared to the adsorption efficiencies of mono-cationic systems, indicating competition on similar active centers (homogeneity substrates). Competition between the different metal ions for surface sites occurs and is dependent on the characteristics of the ions, substrate (crystalline phases, and morphological changes), respectively.

The adsorption isotherms and kinetic data fitted well the Langmuir and pseudo-second order kinetic models, respectively.

The affinities order of ZCR40 for the divalent metal ions reported is $Cu^{2+} > Cd^{2+} > Ni^{2+}$ at optimized contact time 90 min., substrate dose 7g ZCR40/L from multicomponent solution.

This adsorbent material (ZCR40) presents several advantages such as high specific surface area, uniform pore distribution, thermal and mechanical stability, high adsorption capacity, and high fictionalizations ability.

The zeolitic material ZCR40 can be recommended for technologic wastewater treatment.

Acknowledgement

The paper was supported by a grant of the Romanian National Authority for Scientific Research, CNCS – UEFISCDI, project number PNII-RU-TE-2012-3-0177/2013

References

1. Shyam R, Puri JK, Kaur H, Amutha R, Kapila A (2013) Single and multi-binary adsorption of heavy metals on fly ash samples from aqueous solution. Journal of Molecular Liquids 178: 31-36.
2. Tomul F, Basoglu FT (2013) Adsorption of Copper and Zinc from Aqueous Solutions by Bentonite. Asian Journal of Chemistry 22: 615-628.
3. Mimura H, Yokota K, Akiba K (2001) Alkali hydrothermal synthesis of zeolites from coal fly ash and their uptake properties of cesium ion. Journal of Nuclear Science and Technology 38: 766-772.
4. Dieter H (2011) Drinking Water Toxicology in Its Regulatory Framework. Journal of Aquatic Chemistry and Biology 3: 377-415.
5. Wake H (2005) Oil refineries: A review of their ecological impacts on the aquatic environment, Estuarine. Journal of Coastal and Shelf Science 62: 131-140.
6. Visa M, Duta A (2008) Advanced Cd^{2+} Removal on Dispersed TiO_2 – Fly Ash. Journal of Environmental Engineering and Management 7: 373-378.
7. Mata YN, Blázquez ML, Ballester A, González F, Muñoz JA (2009) Sugar beet pulp pectin gels as biosorbent for heavy metals: Preparation and determination of biosorption and desorption characteristics. Chemical Engineering Journal 150: 289-301.
8. Ho YS, McKay G (2004) Sorption of Cooper (II) from aqueous solution by peat. Water Air Soil Pollution 158: 77-97.
9. Šljivić M, Smičiklas I, Pejanović S, Plećaš I (2009) Comparative study of Cu^{2+} adsorption on a zeolite, clay and a diatomite from Serbia. Journal of Applied Clay Science 43: 33-40.
10. Peri J, Trgo M, Medvidovi NV (2004) Removal of zinc, copper and lead by natural zeolite - a comparison of adsorption isotherms. Water Research 38: 1893-1899.
11. Lee MG, YiG, Ahn BJ, Roaddich F (2000) Conversion coal fly ash into zeolite and heavy metal removal characteristics of the products. Korean Journal of Chemical Engineering 3: 325-33.
12. Lee WKW, Deventer JSJ (2002) Structural reorganization of class F fly ash in alkaline silicate solutions. Colloids and Surfaces A: Physicochemical and Engineering Aspects 211: 49-66.
13. Horcas I, Fernandez R, Gomez-Rodriguez JM, Colchero J, Herrero GJ, et al. (2007) WSXM: A software for scanning probe microscopy and a tool for nanotechnology. Rev Sci Instrum 78: 013705.
14. Jha B, Singh DN (2014) A three step process for purification of fly ash zeolites by hydrothermal treatment. Journal of Applied Clay Science 90: 122-129.
15. Garbacz A, Courard L, Kostana K (2006) Characterization of concrete surface roughness and its relation to adhesion in repair systems. Journal of Materials Characterization 56: 281-289.
16. Visa M, Duta A (2013) TiO_2/fly ash as novel substrate for simultaneous removal of heavy metals and surfactants. Journal of Chemical Engineering 223: 860-868.
17. Visa M, Chelaru AM (2014) Hydrothermally modified fly ash for heavy metals and dyes removal in advanced wastewater treatment. Journal of Applied Surface Science 303: 14-22.

18. Martens JA, Jammaer J, Bajpe S, Aerts A, Lorgouilloux Y, et al. (2011) Simple synthesis recipes of porous materials. Journal of Microporous and Mesoporous Materials 140: 2-8.
19. Hui KS, Chao CYH, Kot SC (2005) Removal of mixed heavy metals ions in wastewater by zeolite 4A and residual products from recycled coal fly ash. Journal of Hazardous Materials 127: 89-101.
20. Lagergren S (1898) About the theory of so-called adsorption of soluble substances, Kungliga Svenska Vetenskapsakademiens. Handlingar 24: 39- 41.
21. Ho YS, McKay G (2006) Second-order kinetic model for the sorption of cadmium onto tree fern: a comparison of linear and non-linear methods. Journal of Water Research 40: 119-125.
22. Mohammad I, El- Khaiary, Gihan F, Malash, Ho YS (2010) On the use of linearized pseudo-second-order kinetic equations for modeling adsorption systems. Journal of Desalination 257: 93- 101.
23. Allen SJ, Mc Kay G, Khader ZH (1999) Interparticle diffusion of a basic dye during adsorption onto sphagnum peat. Journal of Environmental Pollution 56: 39-50.
24. Dinu MV, Dragan ES (2010) Evaluation of Cu^{2+}, Co^{2+} and Ni^{2+} Ions removal from aqueous solution using a novel chitosan/clinoptilolite composite kinetics and isotherms. Chemical Engineering Journal 160: 157-163.
25. Liu W, Zhang J, Zhang C, Wang Y, Li Y (2010) Adsorptive removal of Cr(VI) by Fe-modified activated carbon prepared from Trapa natans husk. Chemical Engineering Journal 162: 677-684.
26. Wang S, Li L, Zhu ZH (2007) Solid-state conversion of fly ash to effective adsorbents for Cu removal from wastewater. Journal of Hazardous Materials 139: 254-259.